An Open-Source Toolbox for Automated Removal of Noisy Beats for Accurate Impedance Cardiogram Analysis

Shafa-at Ali Sheikh[1,2], Amit Shah[3], Oleksiy Levantsevych[3], Majd Soudan[3], Jamil Alkhalaf [3], Ali Bahrami Rad[1], Omer T. Inan[2], Gari D. Clifford[1,4]

[1] Department of Biomedical Informatics, Emory University, USA

[2] School of Electrical and Computer Engineering, Georgia Institute of Technology, USA

[3] Rollins School of Public Health, Emory University, USA

[4] Department of Biomedical Engineering, Georgia Institute of Technology and Emory University, USA

E-mail: ssheikh9@gatech.edu

Abstract.

Objective: The impedance cardiogram (ICG) is a non-invasive sensing modality for assessing the mechanical aspects of cardiac function, but is sensitive to artifacts from respiration, speaking, motion, and electrode displacement. Electrocardiogram (ECG)-synchronized ensemble averaging of ICG (conventional ensemble averaging method) partially mitigates these disturbances, as artifacts from intra-subject variability (ISVar) of ICG morphology and event latency remain. This paper describes an automated algorithm for removing noisy beats for improved artifact suppression in ensemble-averaged (EA) ICG beats.

Approach: Synchronized ECG and ICG signals from 144 male subjects at rest in different psychological conditions were recorded. A "three-stage EA ICG beat" was formed by passing 60-seconds non-overlapping ECG-synchronized ICG signals through three filtering stages. The amplitude filtering stage removed spikes/noisy beats with amplitudes outside of normal physiological ranges. Cross-correlation was applied to remove noisy beats in coarse and fine filtering stages. The accuracy of the algorithm-detected artifacts was measured with expert-identified artifacts. Agreement between the expert and the algorithm was assessed using intraclass correlation coefficients (ICC) and Bland-Altman plots. The ISVar of the cardiac parameters was evaluated to quantify improvement in these estimates provided by the proposed method.

Main results: The proposed algorithm yielded an accuracy of 96.3% and high inter-rater reliability (ICC > 0.997). Bland-Altman plots showed consistently accurate results across values. The ISVar of the cardiac parameters derived using the proposed method was significantly lower than those derived via conventional ensemble averaging method ($p < 0.0001$). Enhancement in resolution of fiducial points and smoothing of higher-order time derivatives of the EA ICG beats were observed.

Significance: The proposed algorithm provides a robust framework for removal of noisy beats and accurate estimation of ICG-based parameters. Importantly, the methodology reduced ISVar of cardiac parameters. An open-source toolbox has been provided to enable other researchers to readily reproduce and improve upon this work.

1. Introduction

Impedance cardiography, also known as thoracic electrical bioimpedance, is a non-invasive, safe, and cost-effective technique used to evaluate cardiac function by measuring the electrical impedance of the thorax. The impedance cardiogram (ICG) signal is the first-order time derivative of the thoracic impedance ($\frac{dZ}{dt}$) Patterson (1989). ICG has been found effective in diagnosis and management of hypertension, cardiovascular diseases (heart failure, valvular heart diseases, myocardial infarction), and in postoperative cardiac surgery. Other important clinical applications of the ICG signal include atrioventricular-delay optimization, hemodialysis, and evaluation of optimal settings of the pacemakers Hadidi et al. (2018).

The cardiac functions measured via ICG include hemodynamic parameters related to blood flow (stroke volume (SV), cardiac output (CO)), left ventricular chamber contractility (pre-ejection period (PEP), left ventricular ejection time (LVET), inter-systolic time interval (ISTI)) and other derived arterial properties. (Kubicek (1966)). The calculation of the hemodynamic parameters hinges upon accurate identification of fiducial points in ICG. The critical fiducial points include B, C, and X, which indicate the opening of the aortic valve, maximum ejection velocity, and closing of aortic valve respectively. However, detection of these fiducial points becomes more challenging in the presence of artifacts induced by respiration, body movements, and electrode displacement (Sherwood et al. (1990)). Noisy data can be discarded by visual inspection which requires substantial time and effort, and is subjective. Therefore, there is a need for automatic algorithms enabling the removal of artifacts in the ICG signal.

To remove artifacts from ICG recordings several signal processing techniques have been utilized previously including infinite impulse response (IIR) band-pass filtering (Yamamoto et al. (1988), Savitzky-Golay filtering (Moissl et al. (2003)), moving window technique using linear regression analysis (Eiken and Segerhammar (1988), matched filtering (Nagel et al. (1989)), time-frequency analysis (Wang et al. (1995)), adaptive filtering (Barros et al. (1995),Pandey et al. (2011),Hu et al. (2014)), and wavelet transforms (Pandey and Pandey (2007), Sebastian et al. (2011), Chabchoub et al. (2016), Stepanov et al. (2017)). However, most of the research related to denoising and analysis of ICG relies upon ensemble averaging (Kelsey et al. (1998), Lozano et al. (2007)).

Kizakevich et al. (1976) applied the technique of ensemble averaging on ICG signals to determine systolic time intervals by detecting the R peak of the synchronized ECG signal and using it as a reference point for averaging both ECG and ICG signals over several cardiac cycles. In this paper, we refer to this technique as "conventional ensemble averaging method". Later on, Gollan et al. (1978) verified the technique by measuring systolic time intervals during exercise. By measuring CO using ensemble-averaged (EA) ICG signals, Muzi et al. (1985) established its validity for critically ill patients. Qu et al. (1986) recommended the replacement of band electrodes with spot electrodes using EA ICG signals. Kelsey and Guethlein (1990) recommended 60 s sampling interval for generating EA ICG beat after comparing several hemodynamic parameters derived from

EA ICG signals to beat-to-beat averaging over 60 s and 20 s sampling intervals.

Hurwitz et al. (1993) introduced "coherent ensemble averaging" after identifying that conventional ensemble averaging is susceptible to "intrasubject variability of signal shape and event latency". Coherent ensemble averaging requires marking of fiducial points B, C, and X on a beat-to-beat basis and generation of templates for EA ICG beats and these critical fiducial points. A matching filtering technique was employed to detect signal events of incoming ICG beat by calculating cross-correlation with the templates. This technique was applied to 30 s intervals of 16 subjects under conditions of rest, public speaking, and bicycle exercise.

Kelsey et al. (1998) analyzed the reliability of the EA ICG using conventional scoring and streamlined scoring methods for 1 min baseline rest and 1 min psychological test conditions over 36 subjects. In the conventional scoring method, EA ICG beats were generated after the removal of noisy ICG beats via review/editing of the waveform beat by beat. However, in the streamlined scoring method, EA ICG beats were formed without beat-to-beat review/editing. Based on the apparent equivalence of intersubject means and standard deviations (SDs) of EA ICG measures (RC, RB, ejection velocity $((\frac{dZ}{dt})_{\max})$, etc) for both methods, conventional ensemble averaging without beat-to-beat review/editing was recommended. Moreover, the concept of large scale ensemble averaging based on conventional ensemble averaging for ambulatory ICG was introduced by Riese et al. (2003).

Cybulski et al. (2007) and Cybulski et al. (2011) concluded that in addition to body movements, speaking can also distort the ICG signals. They also refuted the conclusion made by Kelsey et al. (1998) that "variations in beat-to-beat editing do not constitute a serious source of error in the EA ICG". For ambulatory ICG, Cybulski et al. (2017) used PEP, LVET, RR, and $(\frac{dZ}{dt})_{\max}$ for detecting artifacts in ICG signals.

Cieslak et al. (2018) proposed a "moving ensemble average" method for the removal of noisy beats in the ICG signal. In this method "a weighted ensemble average is calculated in a fixed window around each heartbeat". Different window functions (linear, Hann, and Blackman) can be utilized with different window lengths. The technique was applied on 2 min responses to the Valsalva maneuver.

The Physio data toolbox version 0.4 used normalized root mean squared deviation (NRMSD), to identify noisy ICG beats. The metric is calculated between each samples of ICG beats and a corresponding samples of EA ICG beats Sjak-Shie (2018).

"Activity index (AI)-based ensemble averaging" of the ICG signal was introduced by Forouzanfar, Baker, Colrain, Goldstone and de Zambotti (2019), where AI is SD of normalized ICG cycles, with median ICG signal amplitude as a normalization factor. AI thresholds for removal of noisy ICG beats were developed by detecting movement and electrode displacement artifacts from three subjects which were not included in the rest of the study. After removing artifacts, ensemble averaging was performed over 30 s. This method was applied on 20 subjects under different sleep stages. 2000 ICG beats were randomly selected and visually scored by the experts. AI-based ensemble averaging algorithm achieved 87% accuracy in the detection of noisy ICG beats. The

major limitation of this work, as highlighted by the authors, is its inability to detect ICG beats with invalid shape.

The AI-based ensemble averaging algorithm was further refined to "pulse similarity (PS)-based ensemble averaging algorithm" by Forouzanfar, Baker, Colrain and de Zambotti (2019). A new similarity index has been defined as a weighted combination of the four parameters which include AI, structural similarity index, Euclidean norm index, and cross-correlation. An ICG cardiac cycle template was generated by averaging 100 clean ICG beats from three subjects which were not included in the rest of the study. The template has been used to compute all the above-listed parameters except AI. This algorithm was applied to 20 subjects under different sleep stages. 2000 ICG beats were randomly selected and visually scored by the experts. Although this algorithm has achieved 96% accuracy in the detection of noisy ICG beats, it is dependent upon ICG cardiac cycle template derived from three subjects and utilizes weighted combination of four parameters.

In this work, we describe an automatic algorithm for the removal of noisy ICG beats with invalid size and/or shape to form a noise-free EA ICG beat. The algorithm is independent of ICG cardiac cycle template and based on cross-correlation only. It has been tested on 144 subjects under rest in different psychological conditions.

2. Method

2.1. Dataset

This study was performed as an ancillary project on data from the work, "Posttraumatic Stress Disorder and Ischemic Heart Disease: A Longitudinal Twin Study," which examines the relationship between psychological stress and heart disease. The work was approved by the Emory Institutional Review Board. We analyzed data from 144 male participants with ages between 61 and 72 years having mean (SD) of 68 (2.5). Written informed consent was obtained from each subject prior to the study.

Synchronized ECG and ICG signals were recorded by trained researchers at Emory University using impedance and electrocardiography equipment from BIOPAC (BIOPAC Systems Inc., Goleta, CA). For ECG signal recording, two disposable electrodes (3M red dot electrodes) were attached to the collar bone, with a ground electrode located on the hip.

The ICG signal was recorded using NICO100C which was wired to the subject via the MP150 polygraph and four disposable spot electrodes EL507. Outer current electrodes (one at the side of the neck and one at the left lateral side of the thorax below the xiphisternal junction) have been used for injection of alternating current of 400 μ A at 50 kHz frequency. Inner voltage electrodes (one at the side of the neck below the current electrode and one at the left lateral side of the thorax at the xiphisternal junction) were used for voltage pick up. Both ECG and ICG signals were sampled at 1000 Hz with a resolution of 16 bits. Acknowledge 5.0 was used to store, display, and

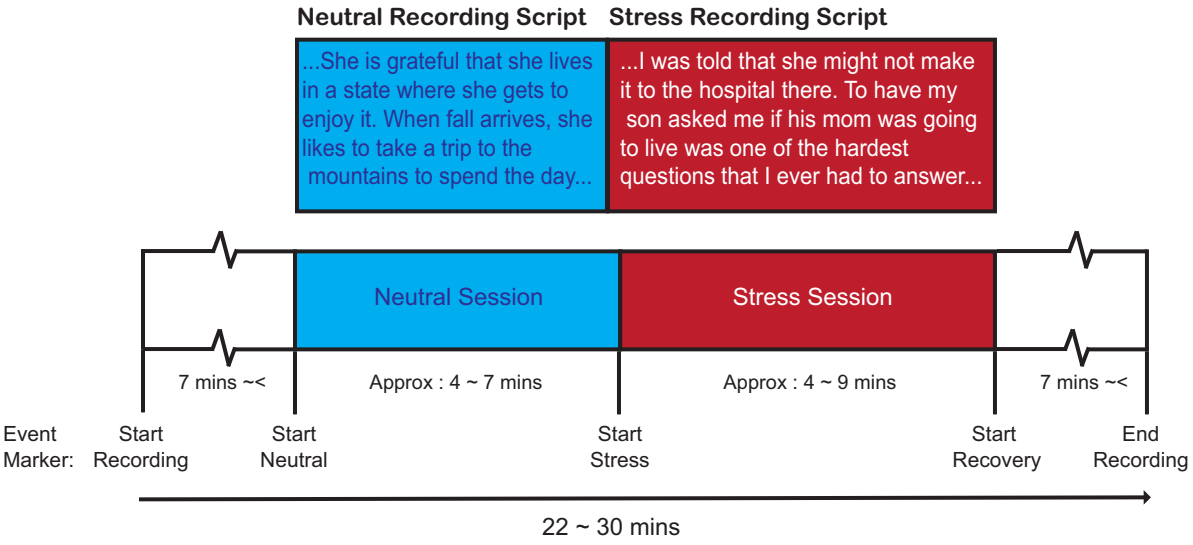

Figure 1: Study protocol timeline. Data recording of 22 to 30 min duration is depicted by event markers "Start Recording" and "End Recording". Neutral Session, represented by a blue box, is approximately 4 to 7 min long and marked by "Start Neutral" and "Start Stress". Stress session depicted by a red box and marked by "Start Stress" and "Start Recovery" markers is approximately 4 to 9 min long. The subjects listened to neutral and stress recording scripts in the respective sessions followed by question-answer episode.

export the data in .mat format. Further analysis and development of the algorithm were carried out in MATLAB R2017b (MathWorks, Inc., Natick, MA).

The subjects were seated in an armchair for the duration of the data recording. The study was divided into neutral and stress sessions. In the neutral session, the subjects listened to two neutral scripts each followed by a short question-answer period. For the stress session, the subjects listened to two stressful recordings (incidents from the subject's own life) followed by a short question-answer period. The neutral session was approximately 4 to 7 min long and the stress session was 4 to 9 min. Figure 1 depicts the study protocol timeline along with an example of scripts for neutral and stress recordings. In this paper, we refer to complete data (neutral and stress sessions) for each subject as "data set", and data for each session as "record". For 144 subjects, we have 144 data sets. Each data set has neutral and stress records which resulted in the availability of 288 records for analysis.

2.2. Preprocessing

Figure 2 represents the signal flow for the processing of simultaneously recorded ECG and ICG signals for the proposed algorithm. The signals recorded from the subject were digitized using an MP150 polygraph. The digitized ECG signal was band-pass filtered with lower and upper cutoff frequencies of 0.5 Hz and 35 Hz respectively by hardware

filters in ECG100C. R peaks were detected in 60 s non-overlapping ECG signals using an open-source toolbox developed by Vest et al. (2018). In this paper, we will refer to the "non-overlapping window of 60 s" as "analysis window". Median RR interval of analysis window of ECG signal was used for ensemble averaging of the ECG signals.

The digitized ICGs were band-pass filtered with lower and upper cutoff frequencies set to 0 and 100 Hz by hardware filters in NICO100. Moreover, in the software processing stage, the ICGs were further filtered using a 4th-order Butterworth band-passed filter to remove low-frequency drift and high-frequency noise. The lower and upper cutoff frequencies were 0.5 Hz and 40 Hz respectively. To avoid phase shift, the Butterworth filter was applied in both forward and backward directions Forouzanfar et al. (2018). ICG signal in an analysis window and R peaks detected from the synchronized analysis window of ECGs are fed into the "Noise Removal Algorithm" for generating the three-stage EA ICG beat.

2.3. Noise Removal Algorithm

The flow chart of the noise removal algorithm is depicted in figure 3. ICG beats in an analysis window are synchronized with R peaks extracted from the simultaneously recorded ECG signal. The length of each ICG beat has been set equal to the median RR interval of the ECG analysis window with a start point equal to "R peak minus 150 ms", and end point equal to the "start point plus the median RR interval". The ICG beats with the median RR interval length in an analysis window are the output of the slanted rectangle box in figure 3, which will undergo three filtration stages.

"Amplitude Filtering" is the first stage of noise removal algorithm, in which spikes and noisy beats are removed based on the maximum and minimum amplitude. Following thresholds defined by Cybulski et al. (2017), any beat with maximum amplitude outside of the range 0.4 to 3 Ωs^{-1} will be discarded. In addition to this, any beat with minimum amplitude less than -2 Ωs^{-1} will also be deleted to handle negative spikes.

The second stage of the proposed algorithm is called "Coarse Filtering". In this stage, all beats passing the amplitude criteria test are accumulated and the ensemble average of these beats is calculated. We may denote this EA ICG beat as "the first stage EA ICG beat". Cross-correlation of the first stage EA ICG beat and each beat after amplitude testing is evaluated to find out their lag and correlation coefficients. Any beat having $\mid Lag \mid \geq 50$ ms OR correlation coefficient ≤ 0.5 is declared noisy and deleted.

The third stage of the noise removal algorithm is "Fine Filtering ". In this stage, all beats passing the coarse filtering criteria test are accumulated and the ensemble average of these beats is calculated. We may denote this EA ICG beat as "the second stage EA ICG beat". Cross-correlation of the second stage EA ICG beat and each beat after the coarse filtering stage is evaluated to find out the lag. Any beat with $\mid Lag \mid \neq 0$ is circularly shifted by the same amount of lag value. Circularly-shifted and zero-lag beats are accumulated. Cross-correlation of the second stage EA ICG beat

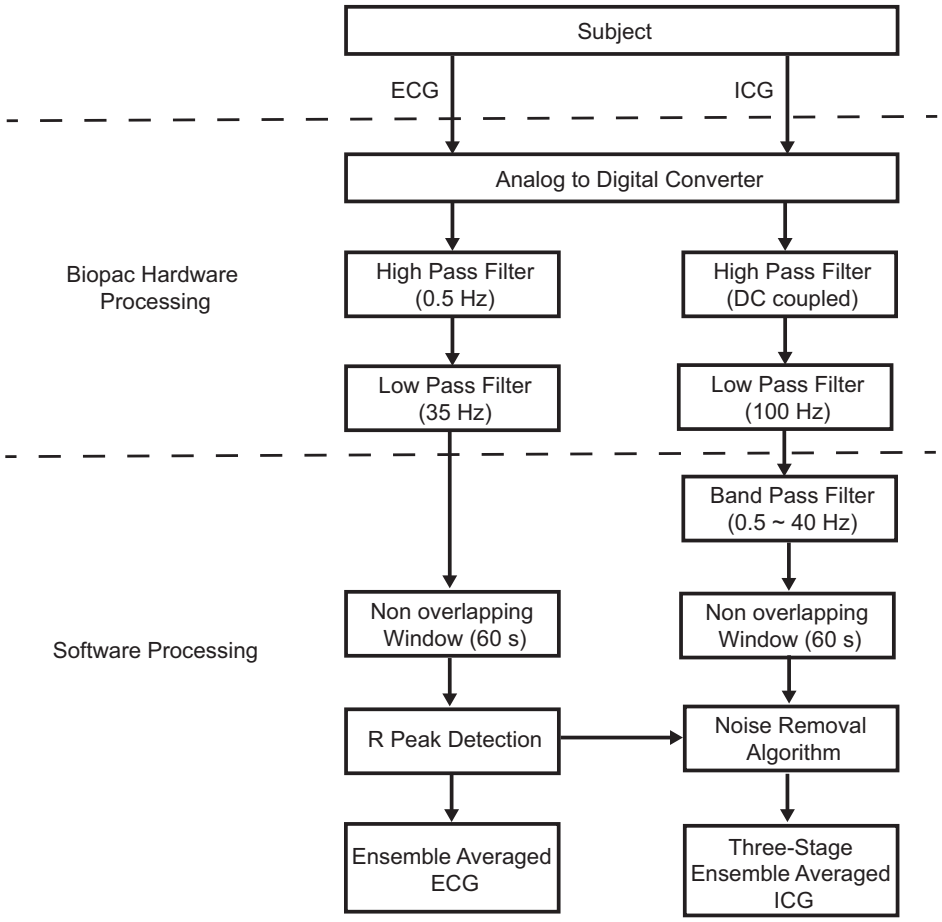

Figure 2: Signal processing for the proposed algorithm. Simultaneously recorded ECG and ICG signals from the subject were digitized and band-pass filtered. The lower and upper cutoff frequencies were set to 0.5 Hz and 35 Hz for ECG signal, and 0 Hz and 100 Hz for ICG signal. In the software processing stage, the ICG signal was further band-pass filtered with lower and upper cutoff frequencies of 0.5 and 40 Hz respectively. R peaks detected over 60 s non-overlapping window (analysis window) of ECG signal were used to form EA ECG. ICG signal in synchronized analysis window and the R peaks were fed into the "Noise Removal Algorithm" to form "three-stage EA ICG".

and accumulated beats is evaluated. All beats having $\mid Lag \mid \leq 1$ ms AND correlation coefficient ≥ 0.8 are declared clean beats. Finally, the clean beats from "Fine Filtering" stage are accumulated and used to evaluate EA ICG beat which will be called the "three-stage EA ICG beat".

2.4. Evaluation method

A random selection of 2500 ICG beats was made to compute accuracy, sensitivity, specificity, Positive Predictive Value (PPV), and F1 score (F1) to evaluate the performance of the algorithm.

The inter-rater reliability between the proposed algorithm and the expert has been

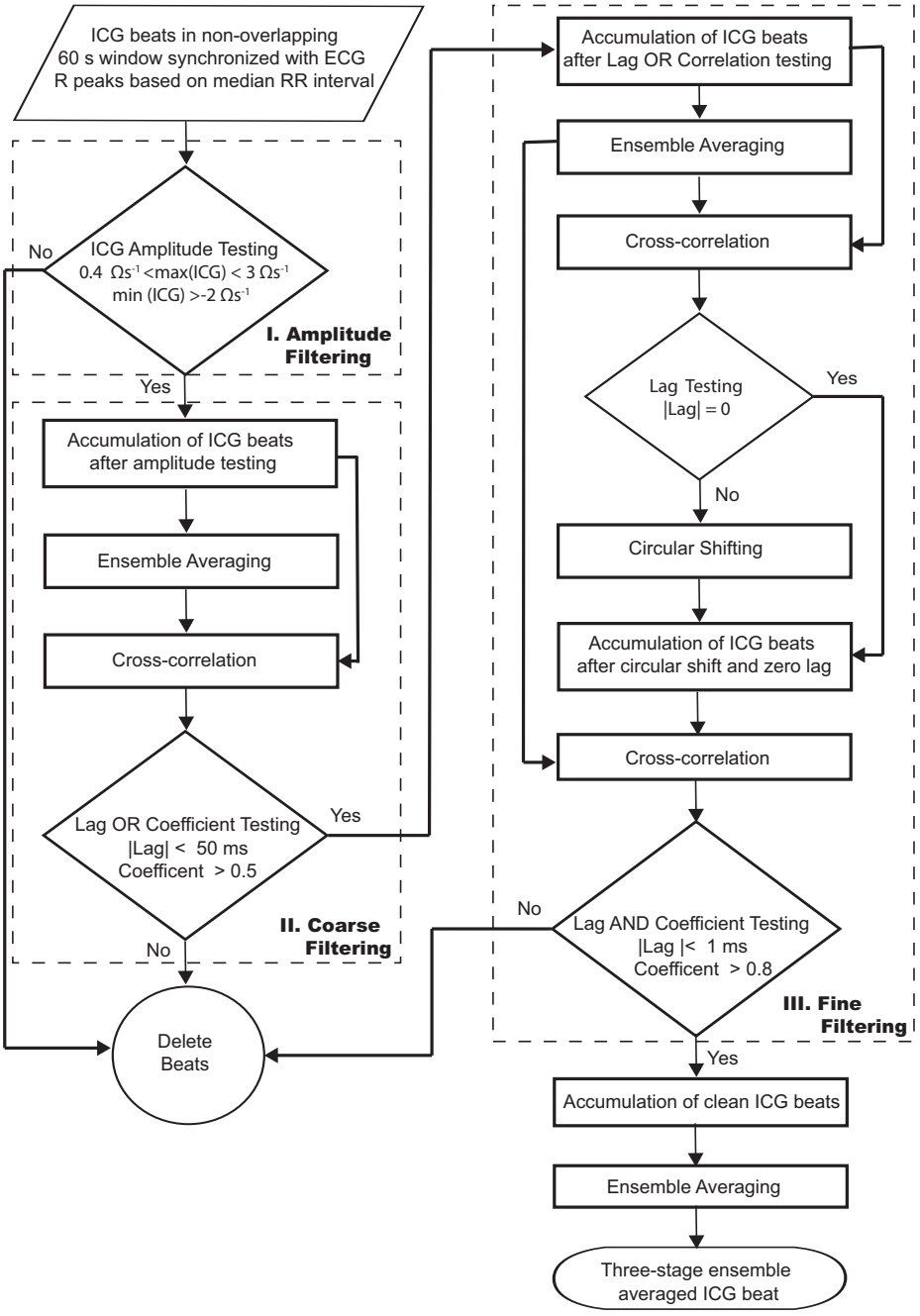

Figure 3: Noise removal algorithm for deriving a three-stage EA ICG beat. The algorithm is represented using different shapes: (1) slanted rectangle for the input data, (2) rectangle/circle for processes, (3) diamond for decisions, and (4) round-edged rectangle for the final output. The slanted box is the start point of the algorithm and contains ICG beats in an analysis window from figure 2. ICG signal has been filtered in three stages: (I) amplitude filtering based on the minimum and maximum amplitude of the C point, (II) coarse filtering based on the lag OR coefficient testing of the ICG beats, and (III) fine filtering based on the lag AND coefficient testing of the circularly shifted ICG beats. The ensemble average of the accumulated clean ICG beats has been taken to generate the three-stage EA ICG beat.

assessed using intraclass correlation coefficients (ICC) based on 2-way random effects absolute agreement model (Model (2,1)) (Shrout and Fleiss (1979) , McGraw and Wong (1996)). For computation of the ICC, the analysis windows from 25 patients in neutral and stress episodes have been randomly selected. The expert-EA ICG beats are generated by removing the expert-identified artifacts. ISTI (RC interval) and PEP (RB interval Seery et al. (2016)) are computed from the expert-EA ICG beats and the three-stage EA ICG beats for inter-rater reliability analysis Brownhill (2020).

Agreement between our proposed algorithm and the expert has also been assessed using Bland-Altman plots for ISTI and RB intervals computed from the 25 patients in neutral and stress episodes Bland and Altman (1986).

A new parameter, "Beat Contribution Factor (BCF)", has been defined for each three-stage EA ICG beat to ascertain its validity for further analysis. BCF is calculated as the ratio of the number of clean beats (output of the third stage of the noise removal algorithm) to the total number of beats in an analysis window (input to the noise removal algorithm). BCF can take on any value from 0 to 1, where values close to 0 indicate that very few clean beats in the analysis window contributed towards forming the three-stage EA ICG beat. BCF value equal to 1 indicates that no noisy beat has been detected by the proposed algorithm. Following Tukey's method for detection of outliers Tukey (1976), a three-stage EA ICG beat is considered as an outlier if its BCF value does not lie in the interval given by lower and upper fence $[(\mathrm{Q1} - 1.5 * \mathrm{IQR}), (\mathrm{Q3} + 1.5 * \mathrm{IQR})]$, where Q1, Q3, and IQR are the first quartile, third quartile, and difference between third and first quartile of BCF values respectively.

At the record level, the intrasubject variability of ISTI, PEP, and ejection velocity index $((\frac{dZ}{dt})_{\max})$ derived using our proposed method has been compared with those derived via conventional ensemble averaging using Wilcoxon signed-rank test. For RC interval and $(\frac{dZ}{dt})_{\max}$, all valid records of conventional and three-stage EA ICG beats have been compared. However, a comparison of PEP (RB interval) depends upon the presence of a feature in RC interval on ICG beat for detection of B point. For this purpose, records made up of conventional EA ICG beats with following characteristics have been selected: 1) records in which all EA ICG beats have a distinct feature in RC interval for identification of B point and 2) in case, there are some featureless EA ICG beats in a record than that record should have at least three conventional EA ICG beats with features in their respective RC intervals. Also, the ratio of EA ICG beats with features to the total number of EA ICG beats in that record should be ≥ 0.6. PEP (RB interval) of corresponding records made up of three-stage EA ICG beats has also been calculated using the same criteria.

As highlighted in sec 1, presence of artifacts affect accurate identification of fiducial points Sherwood et al. (1990). A comparison of resolution of critical fiducial points (B, C, and X) has also been investigated between conventional and three-stage EA ICG beat. For accurate marking of B point on ICG beat, higher-order time derivatives of ICG signal are required to be computed. One such example is marking B point using zero-crossing from negative to positive of sign $(\frac{d^3Z}{dt^3})$. A comparison has also been made to

see the effect of removal of noisy beats on smoothing of the higher-order time derivative of ICG signal.

An application known as "Impedance Cardiogram Manual Annotation Application (ICMAA)" has been developed to annotate fiducial points on EA ECG and EA ICG beats. ICMAA helped us to analyze intrasubject variability of vital hemodynamic parameters, resolution of fiducial points, and smoothing of higher-order time derivative of ICG. Brief description of ICMAA can be found at Appendix A.

3. Results

BCF values for all three-stage EA ICG beats are represented using histogram and boxplot in figure 4. As per Tukey's method, ICG beats with BCF $\geq$ 0.397 (lower fence) have been considered valid for further analysis. Therefore, 54 EA ICG beats have been declared outliers which forms 3.52% of available data. Also, data sets of two subjects (four records) with double R peaks in their ECGs have been excluded from the study. Therefore a total of 140 data sets (280 records) comprising of 1456 EA ICG beats have been analyzed in this study.

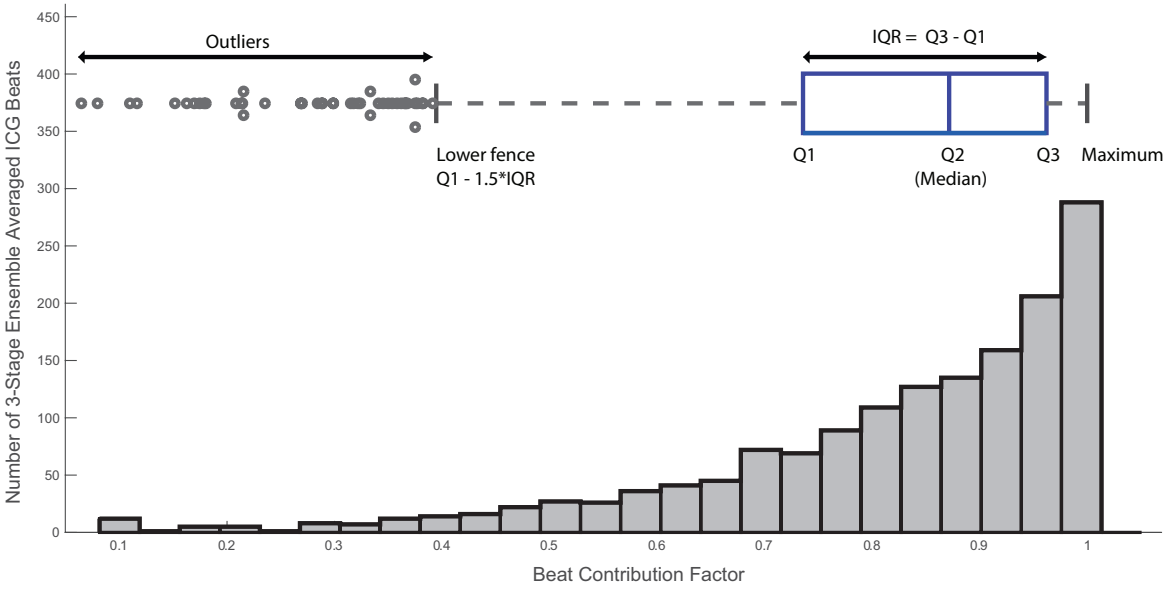

Figure 4: Histogram and boxplot for BCF values of three-stage EA ICG beats. Histogram is left skewed distribution with 1532 observations, mean = 0.82, SD = 0.18, median = 0.872, and mode = 1. The boxplot has Q1 = 0.962, Q2 (median) = 0.872, Q3 = 0.736, IQR (Q3 - Q1) = 0.226, maximum = 1, lower fence = 0.397, and upper fence (not shown) = 1.075. The 54 outliers (3.52% of data) have not been included in the study.

For the calculation of statistical measures, 2500 ICG beats have been randomly selected. Table 1 presents the confusion matrix for the algorithm. An accuracy of 96.28%, sensitivity of 93.18%, specificity of 97.11%, PPV of 89.62% and F1 of 91.36%

were achieved by the proposed algorithm. Examples of noisy ICG beats detected by different filtering stages of the proposed algorithm along with the three-stage EA ICG beat are depicted in appendix Appendix B figure B1.

Table 1: Confusion table for performance analysis of proposed algorithm over 2500 ICG beats.

		Expert		
		Noisy ICG beats	Clean ICG beats	Total
Algorithm	Noisy ICG beats	492 (TP)	57 (FP)	549
	Clean ICG beats	36 (FN)	1915 (TN)	1951
	Total	528	1972	2500

The ICC, presented in table 2, are uniformly high, ranging from 0.9969 to 0.9983 for hemodynamic parameters (ISTI (RC interval) and PEP (RB interval).

Table 2: Intraclass correlation coefficients for PEP and ISTI between the expert and our algorithm for 25 patients. Uniformly high ICC indicate excellent agreement.

Parameter	Intraclass Correlation Coefficent		
	All episodes	Neutral episode	Stress episode
PEP	0.9983	0.9983	0.9983
ISTI	0.9972	0.9969	0.9975

Bland-Altman plots show close agreement between the proposed algorithm and the expert at different PEP and ISTI values across patients. Plots for overall study (neutral and stress episodes) is depicted in figure 5, whereas plots for different study stages are discussed in Appendix C.

Comparison has been made between the intrasubject variances of the hemodynamic parameters (ISTI, PEP and ejection velocity $((\frac{dZ}{dt})_{\max})$) extracted from all records made up of conventional and three-stage EA ICG. The difference in the variances for all three parameters do not follow a normal distribution. Therefore, Wilcoxson signed-rank test has been performed, which indicated that the intrasubject variability of these parameters derived using the proposed method is significantly lower than those derived via the conventional ensemble-averaging method. The results for all records, neutral-episode records and stress-episode records are enumerated in table 3.

Enhancement in feature resolution for all vital fiducial points has also been observed for three-stage EA ICG. Conventional and three-stage EA ICG beats are depicted in figure 6. BCF for the three-stage EA ICG is 0.69. It is evident from the figure that there is marked enhancement in the resolution of fiducial points (B, C, and X) for the three-stage EA ICG beat as compared to conventional EA ICG beat. Removal of noisy beats also resulted in smoothing of the higher-order time derivatives of ICG which facilitates in B point annotation on ICG. An example is discussed in Appendix D.

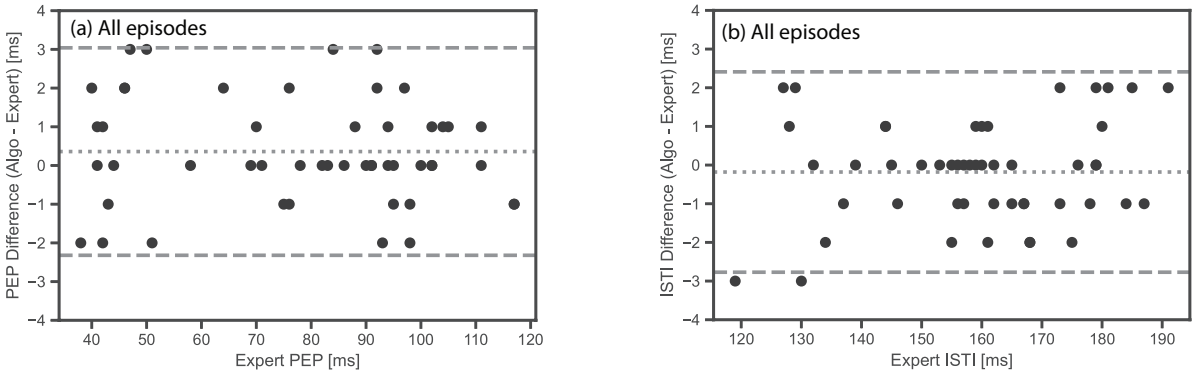

Figure 5: (a) Bland Altman plots for PEP difference between the proposed algorithm and the expert estimates against the expert PEP for all episodes. (b) Bland Altman plots for ISTI difference between the proposed algorithm and expert estimates against the expert ISTI for all episodes. The horizontal dotted line shows the bias(mean of the difference).The horizontal dashed lines show the limits of agreement (bias ± 1.96*SD). All plots show close agreement between the expert and our proposed algorithm at different PEP and ISTI values across patients.

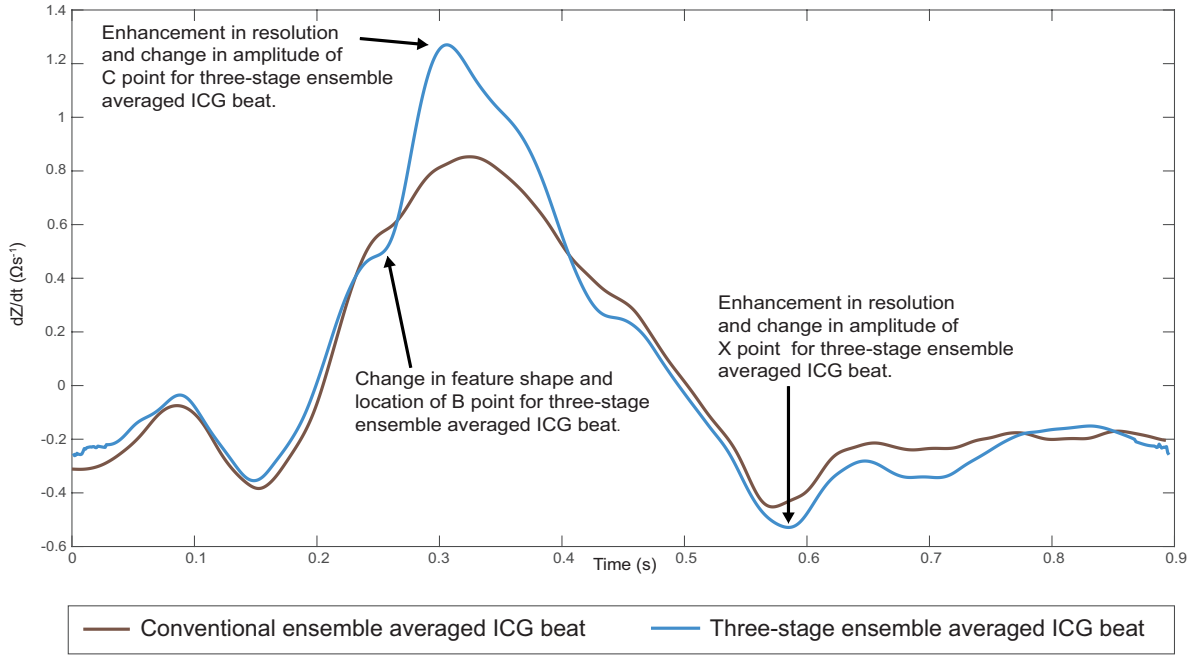

Figure 6: Enhancement of resolution of fiducial points for three-stage EA ICG beat. conventional and three-stage EA ICG beats for the same analysis window have been shown in this figure. Enhancement in resolution and change in location/amplitude of all important fiducial points (B, C, and X) has been found in the three-stage EA ICG beat.

Table 3: Comparison of intrasubject variability of hemodynamic parameters between three-stage and conventional EA records. Based on the presence of a feature in RC interval for detection of B point, the number of records for intrasubject PEP variability analysis are 154 (all episodes analysis), 83 (neutral-episodes analysis), and 71 (stress-episodes analysis). The number of records for intrasubject variability analysis for ISTI and ejection velocity are 280 (all episodes analysis), 140 (neutral-episodes analysis), and 140 (stress-episodes analysis). The mean and SD of all three cardiac parameters evaluated for records obtained from the noise removal algorithm have been found significantly lower than those derived from conventional EA algorithm.

		Noise Removal Algorithm	Conventional EA Algorithm	Wilcoxon Rank Test
Parameters	Records	Mean (SD)	Mean (SD)	P value
All episodes analysis				
PEP	154	12.23 (18.27)	25.92 (69.53)	1.17E-07
ISTI	280	47.25 (157.02)	78.54(243.05)	1.17E-7
Ejection velocity	280	0.004 (0.006)	0.006(0.009)	3.6E-07
Neutral-episodes analysis				
PEP	83	11.61 (19.94)	21.21 (35.44)	1.01E-05
ISTI	140	52.6 (196.88)	96.45(314.25)	1.01E-05
Ejection velocity	140	0.003 (0.004)	0.005(0.006)	1.26E-06
Stress-episodes analysis				
PEP	71	12.97 (16.22)	31.24 (95.06)	2.50E-03
ISTI	140	41.89(103.33)	60.34(138.46)	2.50E-03
Ejection velocity	140	0.005 (0.008)	0.007(0.01)	1.54E-02

4. Discussion

In this work, we have described an automated algorithm for the removal of noisy beats from the ICG signal to form a three-stage EA ICG beat.

Comparison between the proposed algorithm and the experts has been performed using accuracy statistics, ICC, and Bland-Altman plots. The high accuracy of 96.28 % over a large random sample of ICG signal validates the performance of the algorithm. Also, the depiction of noisy ICG beats along with three-stage EA ICG beat as in figure B1 provides a reference to identify the morphology of noisy ICG beats at different filtration stages. The uniformly high ICC values indicate excellent agreement between the proposed algorithm and the expert for clean cycles Koo and Li (2016). Bland Altman plots also depict close agreement between the proposed algorithm and the expert at different ISTI and PEP values across individuals.

Comparison between the proposed algorithm and the conventional ensemble

averaging method has been performed at the beat level and the record level. BCF has been also introduced to check the validity of the three-stage EA ICG beats for further analysis.

In total, 165 EA ICG beats have BCF equal to 1, which shows that no artifacts have been detected in these cases by the algorithm. Low BCF value for an EA ICG beat may indicate that most of the ICG beats in the respective analysis windows are noisy. Tukey's method helped us to identify 54 outliers having a BCF value < 0.397. These outliers have been found in 32 records, among them, 28 records have either 1 or 2 outlier beats. These outlier EA ICG beats are located in the middle or at the end of the neutral/stress session which coincides with the short question-answer episode after listening to neutral/stress session recording. This indicates that speaking and/or excessive body movements might have temporarily induced noise in these records. Remaining 4 records have almost all outlier EA ICG beats which indicate poor/improper electrode connections. Poor electrode connections might have resulted due to the combination of initial improper attachment of the electrodes to body surface and/or loosening of the electrode connections due to the excessive body movement. Two examples of data sets containing outlier EA ICG beats have been discussed in Appendix E. In addition to the identification of outliers, this added utility of BCF value can help us to ascertain the probable cause of excessive noise in the ICG signal, which can be used to improve the study protocols.

It is highlighted in section 1, that apparent equivalence of "**intersubject**" means and SDs of EA ICG measures for "streamlined" and "conventional" methods led to the recommendation that conventional ensemble averaging without a beat-to-beat review/editing can be utilized for further ICG analysis Kelsey et al. (1998). However, this recommendation does not take into account the "**intrasubject**" variability of the EA ICG measures even though the ICG signal is affected by the intrasubject variability of signal morphology and event latency Hurwitz et al. (1990). The "**Intrasubject variability**" has been compared between conventional and three-stage EA ICG records for ISTI, PEP (RB interval), and $(\frac{dZ}{dt})_{\max}$. It has been found that mean and SD values of these measures for three-stage EA ICG records are less than those derived from conventional EA ICG records. Being statistically significant, this result indicates the effectiveness of the proposed algorithm.

Improvement in the resolution of fiducial points (B, C, and X) for a three-stage EA beat will result in a higher degree of accuracy of basic and derived hemodynamic parameters. Also, zero-crossings from negative to positive of sign$(\frac{d^3Z}{dt^3})$ in the RC interval of all conventional and three-stage EA ICG beats have been checked using ICMAA. Fluctuations in the RC interval of conventional EA ICG beats have been found as multiple zero-crossings from negative to positive of sign$(\frac{d^3Z}{dt^3})$ for 29 records, which render it difficult to accurately annotate B point. However, the proposed algorithm helps in the smoothing of higher-order time derivatives of ICG and facilitates in marking of B point. One such example has been discussed in Appendix D. In addition to the better performance over conventional ensemble averaging algorithm, the proposed algorithm

has obvious advantages over other noise removal algorithms in the literature.

Methods based on template matching proposed by Hurwitz et al. (1993) and Cybulski et al. (2017) depend upon the identification/annotation of fiducial points (at least B, C, and X) and derived hemodynamic parameters before detecting artifacts in the ICG signal. However, the proposed method neither requires annotation of the B and X points nor derivation of hemodynamic parameters before its application. C point has been used by all algorithms in the literature to identify amplitude-based artifacts.

Moving ensemble average method does not address systematic problems such as loose electrode connections. Also, it has not been tested under speech conditions Cieslak et al. (2018). The proposed algorithm detects systematic problems such as loose electrode connections and it has been tested under speech conditions once the subjects are questioned after listening to audio recordings. Also, BCF helps us to determine the probable cause of excessive noise from speaking/movement or loose electrode connection.

NRMSD and AI-based algorithms by Sjak-Shie (2018) and Forouzanfar, Baker, Colrain, Goldstone and de Zambotti (2019) help detect noisy ICG beats based on the size of the ICG cycle only. The shape of ICG cycles is not considered for detecting noisy ICG beats. The proposed algorithm also considers the shape of ICG cycles for detecting noisy ICG beats.

The PS-based algorithm proposed by Forouzanfar, Baker, Colrain and de Zambotti (2019) depends upon the template generated by averaging 100 clean ICG cardiac cycles from three subjects that were not included in the study. This requires manual review/editing of beat to beat waveform of ICG signal. The authors did not report the morphology of the ICG cycle template since ICG cycle waveform morphology displays high intersubject and intrasubject variation. Árbol et al. (2017) mentioned six different shapes (notch, plateau, inflection, change in gradient, the onset of rise, featureless) of features in RC interval for identification of the B point. Also, C point exhibit itself in different forms (single peak, double peak (M shape), inflection/valley close to peak) as highlighted by Ermishkin et al. (2014). X point also displays variations in its morphology. It has been identified as the lowest point in the ICG cycle. However, there can be two or more lowest points in close proximity, or there may not be a recognizable X-point at all Sherwood et al. (1990). With so much variation in the morphology of ICG beat, results obtained using a template made from 100 clean cycles of three subjects and tested over 20 subjects could lead to overfitting. Also, template dependency of this algorithm restricts its application. In the proposed algorithm, there is no requirement of manual review/editing of beat to beat waveform in the ICG signal. Also, all stages of the EA ICG beats are subject dependent which addresses the issue of intersubject and intrasubject variability of ICG morphology. In addition, the proposed algorithm works on a single parameter (cross-correlation), however, the PS-based algorithm is based on four parameters.

Although the algorithm described here has displayed better performance over conventional ensemble average methods and other noise removal algorithms, its validity should be tested in the future under exercise and ambulatory conditions on different age

groups. Each ICG beat in an analysis window has a length of the median RR interval, whereas each analysis window is a non-overlapping window of 60 s. The proposed method can also be modified and evaluated for different lengths of the ICG beat and the analysis window. Code for the noise removal algorithm, ICMAA, and ICG-based parameter extraction along with sample data has been provided in the open-source toolbox to enable other researchers to repeat and improve this work.

5. Conclusion

In this study, we sought to create and evaluate an automated ICG signal processing program which would allow for fast and reproducible physiologic analyses that are applicable in various cardiovascular diseases. Our automated algorithm involved the generation of a three-stage EA ICG beat based on a cross-correlation analysis for the removal of noisy ICG beats. Close agreement between the algorithm and expert annotations was demonstrated through ICC and Bland-Altman analysis. Compared to the conventional ensemble averaging method, the proposed algorithm provides a reduction in intrasubject variability, improves the resolution of fiducial points, and smooths higher-order time derivatives of the EA ICG beats. The proposed algorithm also exhibits superior noise reduction performance over other methods in the literature. Future work should examine the behavior of the proposed approach under exercise and ambulatory conditions in which motion artifact is an even larger concern. Notably, this work represents the first open-source toolbox for ICG measurement and can therefore act as a benchmark for other studies, help accelerate the field, and aid reproducibility Sheikh et al. (2020).

Acknowledgements

Shafa-at Ali Sheikh is funded by Fulbright Scholarship Program. The authors wish to acknowledge the National Institutes of Health (Grant # NIH K23HL127251, R01HL136205, R01HL125246, and R03HL146879), the National Science Foundation Award 1636933, and Emory University for their financial support of this research. Any opinions, findings, and conclusions or recommendations expressed in this material are those of the author(s) and do not necessarily reflect the views of the National Institutes of Health, the National Science Foundation, Georgia Institute of Technology and Emory University.

Appendix A. Impedance Cardiogram Manual Annotation Application (ICMAA)

ICMAA has been developed for automatic and manual annotation of fiducial points on ECG and ICG EA beats. Figure A1 depicts the user interface of the application, whereas figure A2 depicts an annotated EA ICG beat with computed hemodynamic parameters.

Automatic R peaks annotation can be simultaneously marked on EA ECG and ICG records using open-source toolbox of Vest et al. (2018). C and X points can also be automatically annotated on EA ICG. B points can be manually annotated based on feature shape (inflection, plateau, notch ,etc) using $\frac{d^3Z}{dt^3}$ and ICG magnitude as per guidelines of Sherwood et al. (1990) and Árbol et al. (2017). The provision of automatic annotation of B point using $(\frac{d^3Z}{dt^3})_{\max}$ for featureless EA ICG beats has also been provided in ICMAA. All fiducial points can also be manually edited. All annotations are automatically saved in text files for each record and can be accessed for further analysis. ICMAA is capable of calculating basic hemodynamic parameters such as ISTI, PEP, LVET, and amplitudes of B, C and X points for current EA ICG beat.

ICMAA has the capability of recording shapes of C peak such as single peak, double peak, flat, and inflection or valley close to the peak. The shape of X point can be saved as single notch, double notch, and not visible. Also feature shape (inflection, plateau, valley, notch, the onset of rise, change in gradient, featureless, invalid or noisy) in RC interval on an EA ICG beat for marking of B point can be recorded. An option of adding notes has also been provided to add special remarks.

Figure A1: GUI for ICMAA. Annotated EA ECG and ICG records being displayed at default data length.

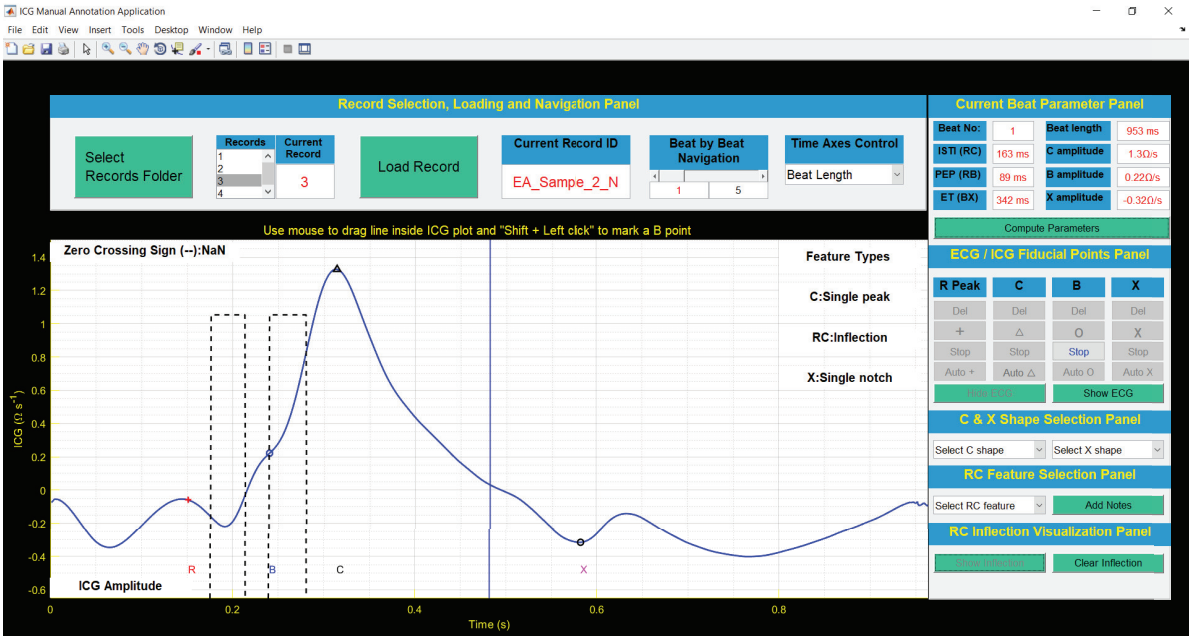

Figure A2: EA ICG beat with fiducial points, feature and hemodynamic parameters. R peak from simultaneously recorded ECG signal has been marked on the EA ICG beat. The highest point in the ICG beat is marked as C point. Feature in RC interval has been identified as Inflection. Zero-crossing of sign $\frac{d^3Z}{dt^3}$ from negative to positive only, depicted as a dashed black vertical line, has been used to identify inflection point in RC interval as B point. X point has been marked as the lowest point of notch after C point. The hemodynamic parameters have been computed using these basic fiducial points and displayed in the Current Beat Parameter Panel. Feature types of C point, RC feature, and X point are marked in the right top corner of the plot.

Appendix B. Noisy ICG beats in three filtration stages

In this section, noisy ICG beats removed at all filtration stages by the proposed algorithm are presented along with the final three-stage EA ICG beat.

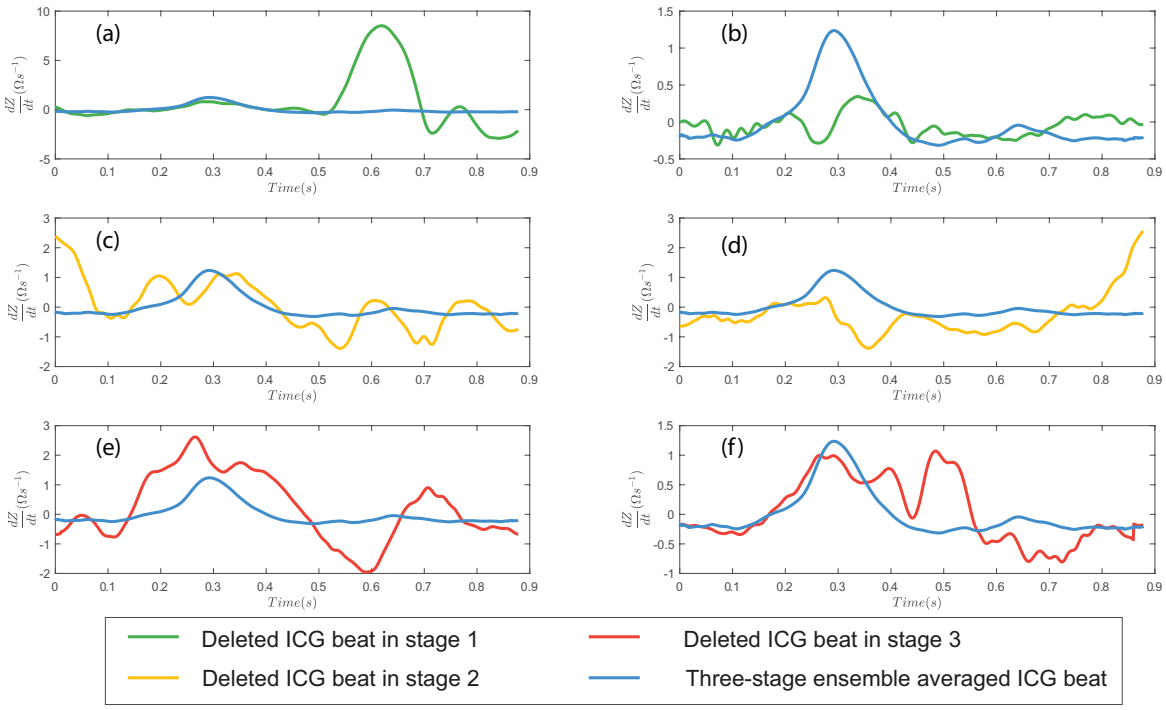

Figure B1: Deleted noisy ICG beats in filtration stages along with three-stage EA ICG beat. Top row: stage 1 (amplitude filtering) - ICG beats with invalid size: (a) Out of limit positive spike (b) C amplitude less than 0.4 Ωs^{-1}. Centre row: stage 2 (coarse filtering) - ICG beats with invalid shape: (c) correlation coefficient < 0.5; (d) absolute(lag) > 50 ms. Bottom row: stage 3 (fine filtering) - ICG beats with invalid shape: both (e) and (f) have correlation coefficient < 0.8 and absolute(lag) > 1 ms .

Appendix C. Agreement analysis between the expert and the proposed algorithm using Bland-Altman plots

Bland-Altman plots depicted in figure C1 show close agreement between the proposed algorithm and the expert at different PEP and ISTI values across patients under different study conditions.

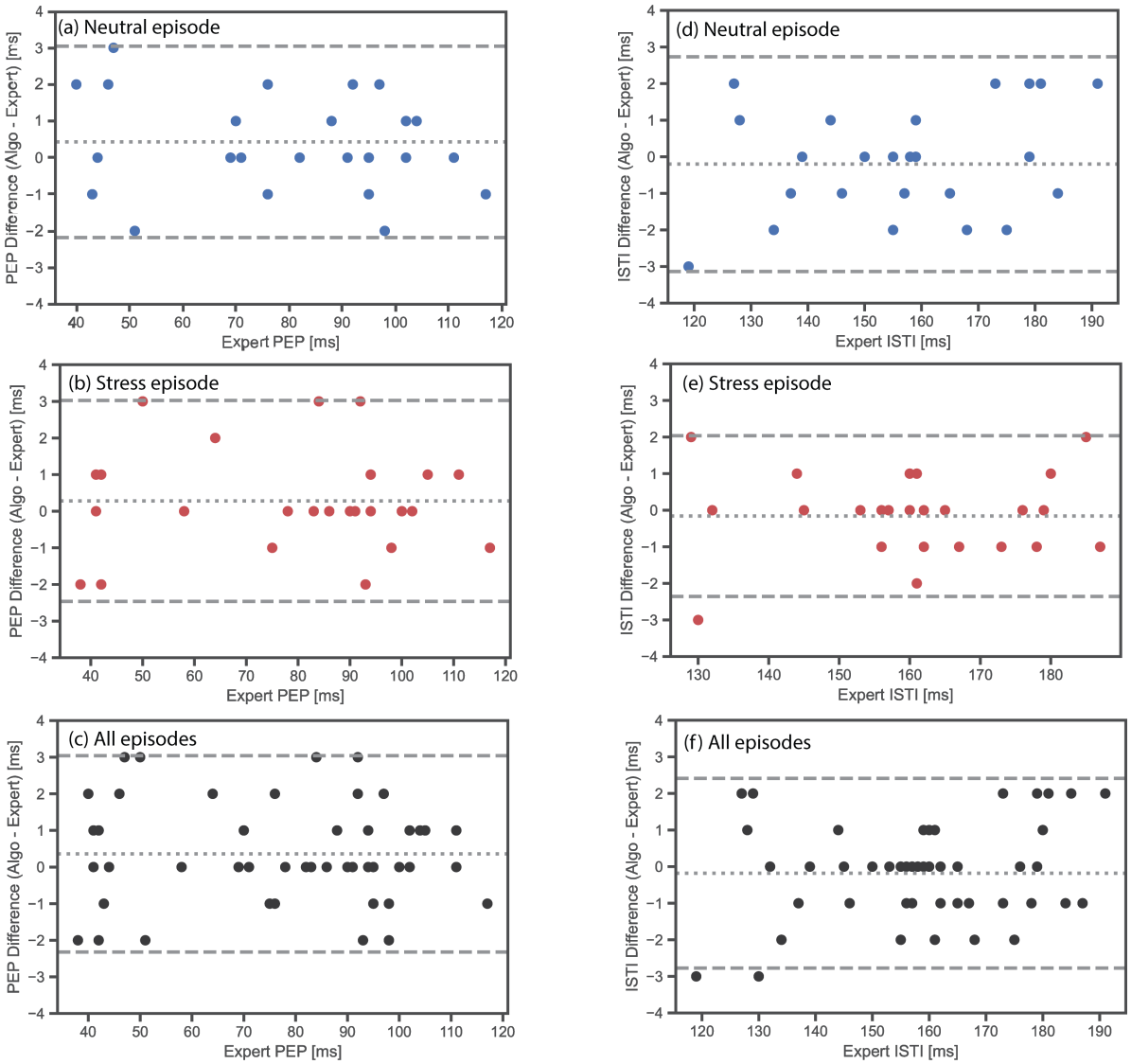

Figure C1: Bland Altman plots for PEP difference between the proposed algorithm and expert estimates against the expert PEP for (a) neutral episode, (b) stress episode, (c) all episodes. Bland Altman plots for ISTI difference between the proposed algorithm and expert estimates against the expert ISTI for (d) neutral episode, (e) stress episode, (f) all episodes. The horizontal dotted line shows the bias (mean of the difference).The horizontal dashed lines show the limits of agreement (bias ± 1.96*SD). All plots show close agreement between the expert and our proposed algorithm at different PEP and ISTI values across patients.

Appendix D. Effect of removal of noisy beats on higher-order time derivatives of EA ICG

B point can be annotated by identifying a feature in the RC interval of ICG beat. "Inflection" and "plateau" are the most recurrent features in the RC interval of ICG beats for annotating B point. Zero-crossing of $\frac{d^3Z}{dt^3}$ in the RC interval of ICG beat gives us the location of B point for these features. In case of absence of feature, $(\frac{d^3Z}{dt^3})_{\max}$) in RC interval is considered B point. Therefore, smooth $\frac{d^3Z}{dt^3}$ is desired for accurate annotation of B points.

By using "RC Inflection Visualization Panel" of ICMAA, user can annotate B point by displaying zero-crossings of $\frac{d^3Z}{dt^3}$. For conventional EA ICG beat (figure D1 (a)), we can see multiple zero crossings from negative to positive in RC interval (figure D1(c)) which represent multiple inflection points to manual annotator as well as any automated B point detection algorithm. However, this problem has been resolved by the proposed algorithm for three-stage EA ICG beat (figure D1 (b)), where a single zero crossing from negative to positive in RC interval (figure D1 (d)) facilitates detection of accurate B point.

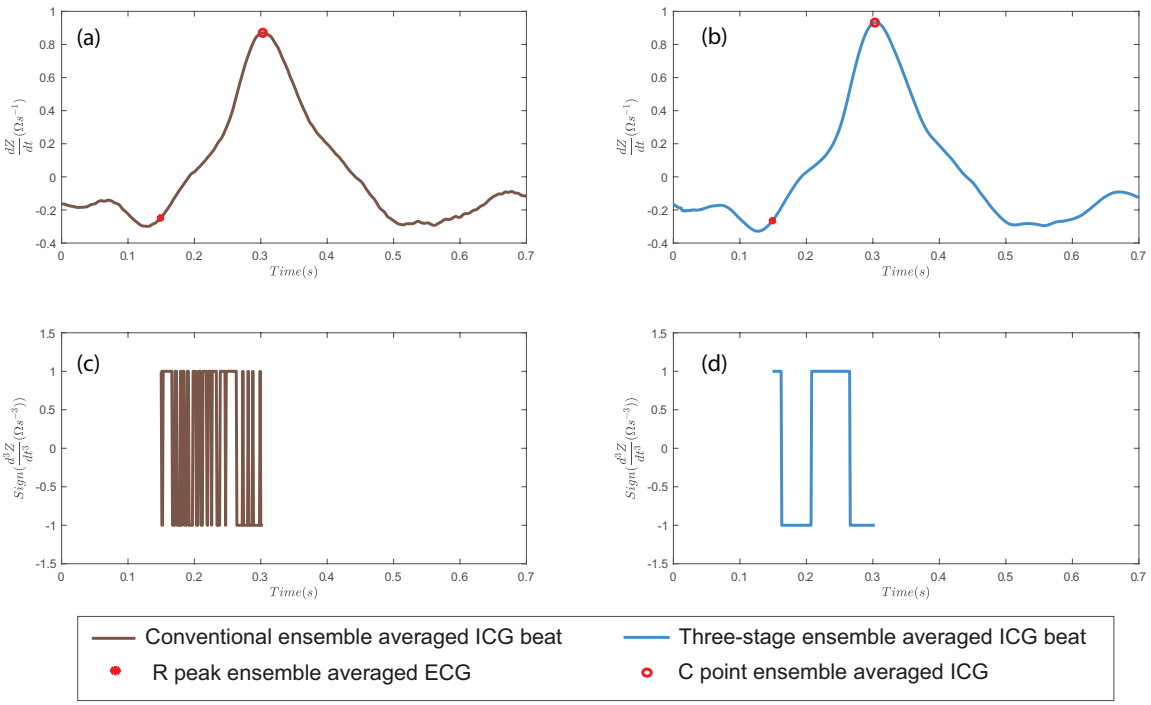

Figure D1: Comparison of fluctuations in RC interval for conventional and three-stage EA ICG beat using $(\frac{d^3Z}{dt^3})$. (a) conventional EA ICG beat. (b) three-stage EA ICG beat. (c) Multiple zero-crossings from negative to positive of sign$(\frac{d^3Z}{dt^3})$ for conventional EA ICG beat makes it difficult to annotate B point. (d) Single zero crossing from negative to positive of sign $(\frac{d^3Z}{dt^3})$ for three-stage EA ICG beat facilitates the accurate marking of B point.

Appendix E. Analysis of data sets with outlier three-stage EA ICG beats

Two data sets containing outlier three-stage EA ICG beats have been analyzed in this section. As depicted in figure E1, three-stage EA ICG beats for 2 subjects have been plotted against their BCF values. A beat will be considered outlier if its BCF value falls under the horizontal threshold line (BCF Threshold = 0.397).

Data set for subject 1 consists of 8 three-stage EA ICG beats where beats 1 and 2 have BCF values close to 1, but BCF values for remaining beats dropped below the threshold. Excessive body movements might have loosened the electrode connections resulting in noisy ICG signals for beats 3 to 8.

Data set for subject 2 consists of 11 EA ICG beats. EA ICG beat number 8 for subject 2 is below the BCF threshold value. This event coincides with the short question-answer episode in stress session, which indicates that noise might have been temporarily induced in this data set due to the combination of speaking and/or body movements.

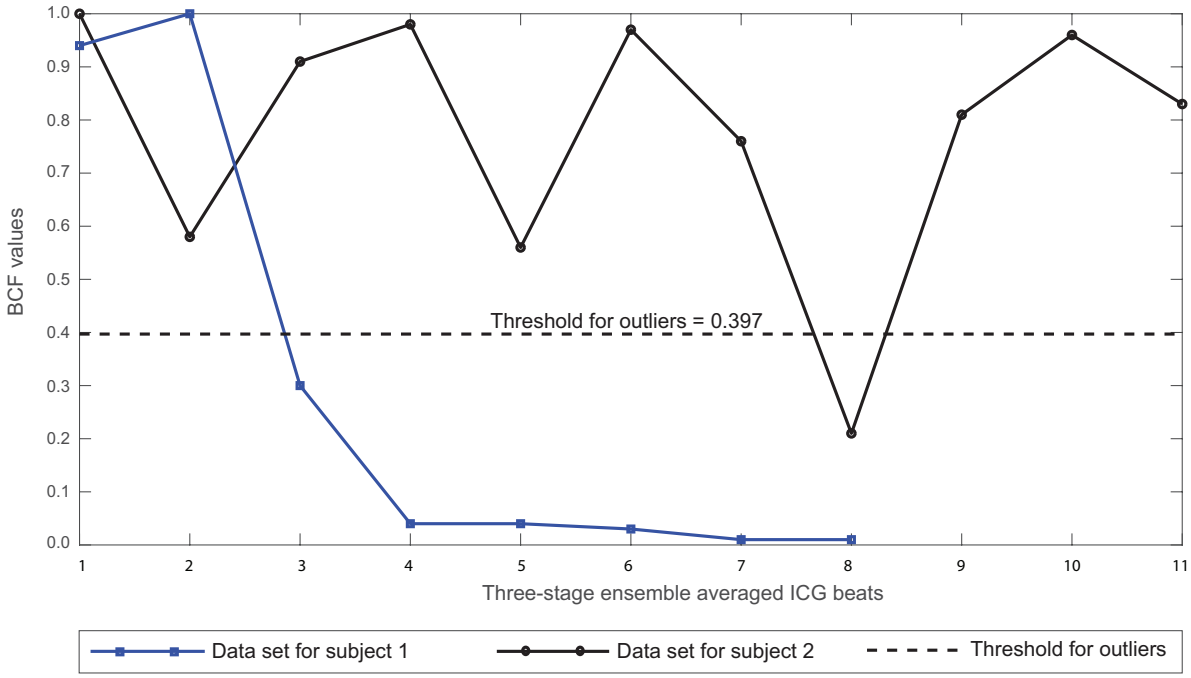

Figure E1: Examples of data sets with BCF based outliers. three-stage EA ICG beats for data set for subject 1 and subject 2 are plotted against their respective BCF values. All beats under the horizontal dashed line at BCF = 0.397 are outliers. For subject 1, the sudden drop in BCF values after beat 2 indicates loosened electrode connections. For subject 2, dip at beat 8 below threshold indicates temporarily induced noise due to excessive speaking/movement.

References

Árbol, J. R., Perakakis, P., Garrido, A., Mata, J. L., Fernández-Santaella, M. C. and Vila, J. (2017). Mathematical detection of aortic valve opening (b point) in impedance cardiography: A comparison of three popular algorithms, *Psychophysiology* **54**(3): 350–357.

Barros, A. K., Yoshizawa, M. and Yasuda, Y. (1995). Filtering noncorrelated noise in impedance cardiography, *IEEE Transactions on Biomedical Engineering* **42**(3): 324–327.

Bland, J. M. and Altman, D. (1986). Statistical methods for assessing agreement between two methods of clinical measurement, *The lancet* **327**(8476): 307–310.

Brownhill, K. (2020). Intraclass correlation coefficients. https://www.mathworks.com/matlabcentral/fileexchange/21501-intraclass-correlation-coefficients, MATLAB Central File Exchange. Accessed on: Apr 2, 2020.

Chabchoub, S., Mansouri, S. and Salah, R. B. (2016). Impedance cardiography signal denoising using discrete wavelet transform, *Australasian physical & engineering sciences in medicine* **39**(3): 655–663.

Cieslak, M., Ryan, W. S., Babenko, V., Erro, H., Rathbun, Z. M., Meiring, W., Kelsey, R. M., Blascovich, J. and Grafton, S. T. (2018). Quantifying rapid changes in cardiovascular state with a moving ensemble average, *Psychophysiology* **55**(4): e13018.

Cybulski, G., Młyńczak, G., Żyliński, M., Strasz, A., Gasiorowska, A. and Niewiadomski, W. (2017). The quality of automatic artifact identification in ambulatory impedance cardiography monitoring, *EMBEC & NBC 2017*, Springer, pp. 165–168.

Cybulski, G., Niewiadomski, W., Aksler, M., Strasz, A., Gasiorowska, A., Laskowska, D. and Pałko, T. (2011). Identification of the sources of artefacts in the holter-type impedance cardiography recordings, *5th European Conference of the International Federation for Medical and Biological Engineering*, Springer, pp. 1272–1274.

Cybulski, G., Niewiadomski, W., Gasiorowska, A. and Kwiatkowska, D. (2007). Signal quality evaluation in ambulatory impedance cardiography, *13th International Conference on Electrical Bioimpedance and the 8th Conference on Electrical Impedance Tomography*, Springer, pp. 590–592.

Eiken, O. and Segerhammar, P. (1988). Elimination of breathing artefacts from impedance cardiograms at rest and during exercise, *Medical and Biological Engineering and Computing* **26**(1): 13–16.

Ermishkin, V., Kolesnikov, V. and Lukoshkova, E. (2014). Age-dependent and pathologicchanges in icg waveforms resulting from superposition of pre-ejection and ejection waves, *Physiological measurement* **35**(6): 943.

Forouzanfar, M., Baker, F. C., Colrain, I. M. and de Zambotti, M. (2019). Automatic artifact detection in impedance cardiogram using pulse similarity index, *2019 41st*

Annual International Conference of the IEEE Engineering in Medicine and Biology Society, IEEE, pp. 2629–2632.

Forouzanfar, M., Baker, F. C., Colrain, I. M., Goldstone, A. and de Zambotti, M. (2019). Automatic analysis of pre-ejection period during sleep using impedance cardiogram, *Psychophysiology* **56**(7): e13355.

Forouzanfar, M., Baker, F. C., de Zambotti, M., McCall, C., Giovangrandi, L. and Kovacs, G. T. (2018). Toward a better noninvasive assessment of preejection period: A novel automatic algorithm for b-point detection and correction on thoracic impedance cardiogram, *Psychophysiology* **55**(8): e13072.

Gollan, F., Kizakevich, P. N. and McDERMOTT, J. (1978). Continuous electrode monitoring of systolic time intervals during exercise., *Heart* **40**(12): 1390–1396.

Hadidi, T. M. A. et al. (2018). Impedance cardiography: recent applications and developments.

Hu, X., Chen, X., Ren, R., Zhou, B., Qian, Y., Li, H. and Xia, S. (2014). Adaptive filtering and characteristics extraction for impedance cardiography, *Journal of Fiber bioengineering and Informatics* **7**(1): 81–90.

Hurwitz, B. E., Shyu, L.-Y., Lu, C.-C., Reddy, S. P., Schneiderman, N. and Nagel, J. H. (1993). Signal fidelity requirements for deriving impedance cardiographic measures of cardiac function over a broad heart rate range.

Hurwitz, B. E., Shyu, L.-Y., Reddy, S. P., Schneiderman, N. and Nagel, J. H. (1990). Coherent ensemble averaging techniques for impedance cardiography, *[1990] Proceedings. Third Annual IEEE Symposium on Computer-Based Medical Systems*, IEEE, pp. 228–235.

Kelsey, R. M. and Guethlein, W. (1990). An evaluation of the ensemble averaged impedance cardiogram, *Psychophysiology* **27**(1): 24–33.

Kelsey, R. M., Reiff, S., Wiens, S., Schneider, T. R., Mezzacappa, E. S. and Guethlein, W. (1998). The ensemble-averaged impedance cardiogram: An evaluation of scoring methods and interrater reliability, *Psychophysiology* **35**(3): 337–340.

Kizakevich, P., McDermott, J. and Gollan, F. (1976). An automated system for systolic time interval analysis, *Proc. Dig. Equip. Users Soc* **2**: 795–798.

Koo, T. K. and Li, M. Y. (2016). A guideline of selecting and reporting intraclass correlation coefficients for reliability research, *Journal of chiropractic medicine* **15**(2): 155–163.

Kubicek, W. G. (1966). Development and evaluation of an impedance cardiac output system, *Aerosp Med* **37**: 1208–1212.

Lozano, D. L., Norman, G., Knox, D., Wood, B. L., Miller, B. D., Emery, C. F. and Berntson, G. G. (2007). Where to b in dz/dt, *Psychophysiology* **44**(1): 113–119.

McGraw, K. O. and Wong, S. P. (1996). Forming inferences about some intraclass correlation coefficients., *Psychological methods* **1**(1): 30.

Moissl, U., Wabel, P. and Isermann, R. (2003). Filtering respiration in impedance cardiography, *IFAC Proceedings Volumes* **36**(15): 371–376.

Muzi, M., Ebert, T. J., Tristani, F. E., Jeutter, D. C., Barney, J. A. and Smith, J. J. (1985). Determination of cardiac output using ensemble-averaged impedance cardiograms, *Journal of Applied Physiology* **58**(1): 200–205.

Nagel, J. H., Shyu, L.-Y., Reddy, S. P., Hurwitz, B. E., McCabe, P. M. and Schneiderman, N. (1989). New signal processing techniques for improved precision of noninvasive impedance cardiography, *Annals of Biomedical Engineering* **17**(5): 517–534.

Pandey, V. K. and Pandey, P. C. (2007). Wavelet based cancellation of respiratory artifacts in impedance cardiography, *Digital Signal Processing, 2007 15th International Conference on*, IEEE, pp. 191–194.

Pandey, V. K., Pandey, P. C., Burkule, N. J. and Subramanyan, L. (2011). Adaptive filtering for suppression of respiratory artifact in impedance cardiography, *2011 Annual International Conference of the IEEE Engineering in Medicine and Biology Society*, IEEE, pp. 7932–7936.

Patterson, R. P. (1989). Fundamentals of impedance cardiography, *IEEE Engineering in Medicine and Biology magazine* **8**(1): 35–38.

Qu, M., Zhang, Y., Webster, J. G. and Tompkins, W. J. (1986). Motion artifact from spot and band electrodes during impedance cardiography, *IEEE Transactions on Biomedical Engineering* (11): 1029–1036.

Riese, H., Groot, P. F., Van Den Berg, M., Kupper, N. H., Magnee, E. H., Rohaan, E. J., Vrijkotte, T. G., Willemsen, G. and de Geus, E. J. (2003). Large-scale ensemble averaging of ambulatory impedance cardiograms, *Behavior Research Methods, Instruments, & Computers* **35**(3): 467–477.

Sebastian, T., Pandey, P. C., Naidu, S. and Pandey, V. K. (2011). Wavelet based denoising for suppression of respiratory and motion artifacts in impedance cardiography, *2011 Computing in Cardiology*, IEEE, pp. 501–504.

Seery, M. D., Kondrak, C. L., Streamer, L., Saltsman, T. and Lamarche, V. M. (2016). Preejection period can be calculated using r peak instead of q, *Psychophysiology* **53**(8): 1232–1240.

Sheikh, S. A., Shah, A., Inan, O. and Clifford, G. D. (2020). Open Source Toolbox for ICG Analysis. v1.0, [online]. Available: https://github.com/cliffordlab/ICG_OSToolbox, Accessed on: Apr 5, 2020.

Sherwood, A., Allen, M. T., Fahrenberg, J., Kelsey, R. M., Lovallo, W. R. and Van Doornen, L. J. (1990). Methodological guidelines for impedance cardiography, *Psychophysiology* **27**(1): 1–23.

Shrout, P. E. and Fleiss, J. L. (1979). Intraclass correlations: uses in assessing rater reliability., *Psychological bulletin* **86**(2): 420.

Sjak-Shie, E. E. (2018). Physiodata toolbox (version 0.4) [computer software]. Retrieved from : https://physiodatatoolbox.leidenuniv.nl.

Stepanov, R., Podtaev, S., Frick, P. and Dumler, A. (2017). Beat-to-beat cardiovascular hemodynamic parameters based on wavelet spectrogram of impedance data, *Biomedical Signal Processing and Control* **36**: 50–56.

Tukey, J. W. (1976). Exploratory data analysis. 1977, *Massachusetts: Addison-Wesley* .

Vest, A. N., Da Poian, G., Li, Q., Liu, C., Nemati, S., Shah, A. J. and Clifford, G. D. (2018). An open source benchmarked toolbox for cardiovascular waveform and interval analysis, *Physiological measurement* **39**(10): 105004.

Wang, X., Sun, H. H. and Van De Water, J. M. (1995). An advanced signal processing technique for impedance cardiography, *IEEE Transactions on biomedical engineering* **42**(2): 224–230.

Yamamoto, Y., Mokushi, K., Tamura, S., Mutoh, Y., Miyashita, M. and Hamamoto, H. (1988). Design and implementation of a digital filter for beat-by-beat impedance cardiography, *IEEE transactions on biomedical engineering* **35**(12): 1086–1090.